Electronic Supplementary Material (ESI) for New Journal of Chemistry.

Cation-Selective and Anion-Controlled Benzothiazolyl-Attached Macrocycle as NLO-based Cation Detection: Variational First Hyperpolarizabilities

Jinting Ye [a], Li Wang [a], Hongqiang Wang [a], Xiumei Pan [a, b], Haiming Xie [a, b], and Yongqing Qiu [a, b, *]

[a] Institute of Functional Material Chemistry, Faculty of Chemistry, Northeast Normal University, Changchun, 130024, China

[b] National & Local United Engineering Laboratory for Power Battery, Faculty of Chemistry, Northeast Normal University, Changchun, 130024, China

[*] Corresponding Author. Fax: +86 431 85098768.
E-mail addresses: qiuyq466@nenu.edu.cn (Y. Q. Qiu).

The electronic density variation between the excited $\rho_{ES}(r)$ and ground states $\rho_{GS}(r)$ are defined as follows:

$$\Delta\rho(r) = \rho_{ES}(r) - \rho_{GS}(r) \tag{1}$$

Subsequently, the function is divided into two categories representing an increase (ρ_+) or a decrease (ρ_-) of the density in space resulting from the electronic transition. Hence the q^{CT} is given as:

$$q^{CT} = \int \rho_+(r)dr = \int \rho_-(r)dr \tag{2}$$

The density distribution barycenters (r_+ and r_-), giving the starting and ending points of transfer, corresponding to ρ_+ and ρ_- are defined by:

$$\begin{aligned} r_+ &= (x_+, y_+, z_+) = \frac{1}{q^{CT}} \int r\rho_+(r)dr \\ r_- &= (x_-, y_-, z_-) = \frac{1}{q^{CT}} \int r\rho_-(r)dr \end{aligned} \tag{3}$$

And d^{CT} is thus defined as the distance separating between the two points (r_+ and r_-), which is an important factor to evaluate the CT length.

$$d^{CT} = \left| r_+ - r_- \right| \tag{4}$$

Eventually, an index H is defined as half of the sum of centroids axis (x axis) along the molecular structure direction.

$$H = \frac{\sigma_{+x} + \sigma_{-x}}{2} \tag{5}$$

If $H \cong d^{CT}$, there is a significant overlap between the centroids along this axis.

Finally, the t index is proposed to evaluate the degree of separation between $\rho_+(r)$ and $\rho_-(r)$ regions.

$$t = d^{CT} - H \tag{6}$$

Large t value indicates less overlap between the regions with an increment or a depletion of the density.

Table S1. Individual components of first hyperpolarizabilities and total first hyperpolarizabilities (10^{-30} esu) of **L** and **L*M** complexes computed at various levels of theory in acetonitrile solution.

Complex	Functionals	β_x	β_y	β_z	β_{tot}	β_{tot} (**L**)/ β_{tot} (**L*M**)
	CAM-B3LYP	125.7	-3.7	0.6	125.8	-
L	ωB97XD	116.1	-3.1	1.0	116.1	-
	M06-2X	133.5	-3.8	0.5	133.5	-
	CAM-B3LYP	97.8	1.0	6.0	98.0	1.3
L*Na$^+$	ωB97XD	90.7	1.5	6.4	91.0	1.3
	M06-2X	102.7	1.2	6.2	102.9	1.3
	CAM-B3LYP	102.2	0.7	7.3	102.4	1.2
L*K$^+$	ωB97XD	94.6	1.2	7.5	95.0	1.2
	M06-2X	107.5	0.8	7.5	107.8	1.2
	CAM-B3LYP	49.0	-2.8	-1.6	49.1	2.6
L*Mg^{2+}	ωB97XD	46.1	-2.3	-0.9	46.1	2.5
	M06-2X	48.9	-2.5	-2.2	49.0	2.7
	CAM-B3LYP	77.6	0.9	5.4	77.8	1.6
L*Ca^{2+}	ωB97XD	72.6	1.6	5.5	72.9	1.6
	M06-2X	81.0	0.9	4.9	81.2	1.6
	CAM-B3LYP	46.5	-3.9	-3.6	46.8	2.7
L*Zn^{2+}	ωB97XD	43.6	-3.3	-2.9	43.8	2.7
	M06-2X	47.7	-3.4	-3.0	48.0	2.8
	CAM-B3LYP	58.9	-3.7	1.9	59.0	2.1
L*Cd^{2+}	ωB97XD	54.8	-3.0	2.5	54.9	2.1
	M06-2X	60.9	-3.4	2.3	61.0	2.2
	CAM-B3LYP	-2.6	6.4	-4.5	8.2	15.3
L*Hg^{2+}	ωB97XD	-3.9	7.6	-5.4	10.1	11.5
	M06-2X	-3.0	6.7	-4.4	8.6	15.5

	CAM-B3LYP	119.5	-2.0	12.1	120.1	1.0
Hg(L)(Cl)$_2$	ωB97XD	110.9	-0.5	12.0	115.7	1.0
	M06-2X	125.1	-0.9	11.1	125.6	1.1
	CAM-B3LYP	38.0	2.0	5.7	38.6	3.3
Hg(L)(ClO$_4$)$_2$	ωB97XD	34.3	2.4	6.0	34.9	3.3
	M06-2X	37.5	1.5	5.2	37.9	3.5

Table S2. The β_{HRS}, β_J and $\Phi(\beta_J)$ values, as well as ρ and DR of complexes **L** and **L*M** calculated at the ωB97XD/6-311+G(d,p)/SDD level in acetonitrile, using wavelengths of 1064, 1340, 1460, 1907 nm and in the static limit (λ=∞).

Complex	β_{HRS}	DR	$\lvert\beta_{J=1}\rvert$	$\lvert\beta_{J=3}\rvert$	ρ	$\Phi(\beta_{J=1})$	$\Phi(\beta_{J=3})$
			λ=1064nm				
L	62.7	4.8	115.8	100.1	0.87	0.54	0.46
L*Na$^+$	51.3	4.8	94.4	82.3	0.87	0.53	0.47
L*K$^+$	53.6	4.7	98.7	86.3	0.87	0.53	0.47
L*Mg^{2+}	27.7	4.46	50.0	47.2	0.94	0.51	0.49
L*Ca^{2+}	41.7	4.7	76.4	68.0	0.89	0.53	0.47
L*Zn^{2+}	27.0	4.4	48.6	46.4	0.95	0.51	0.49
L*Cd^{2+}	33.6	4.5	61.0	56.4	0.92	0.52	0.48
L*Hg^{2+}	2.5	2.6	3.4	6.3	1.85	0.35	0.65
			λ=1340nm				
L	47.8	4.7	87.9	77.3	0.88	0.53	0.47
L*Na$^+$	39.8	4.7	73.0	64.5	0.88	0.53	0.47
L*K$^+$	41.5	4.7	76.1	75.6	0.89	0.53	0.47
L*Mg^{2+}	21.8	4.4	39.0	37.9	0.97	0.51	0.49
L*Ca^{2+}	32.6	4.6	59.5	53.9	0.91	0.52	0.48
L*Zn^{2+}	21.1	4.3	37.7	37.0	0.98	0.50	0.50
L*Cd^{2+}	26.2	4.5	47.3	44.7	0.94	0.51	0.49
L*Hg^{2+}	2.3	2.6	3.1	5.7	1.86	0.35	0.65
			λ=1460nm				
L	44.8	4.7	82.3	72.6	0.88	0.53	0.47
L*Na$^+$	37.4	4.7	68.6	60.9	0.89	0.53	0.47
L*K$^+$	39.0	4.7	71.4	63.7	0.89	0.53	0.47
L*Mg^{2+}	20.5	4.3	36.7	35.8	0.98	0.51	0.49
L*Ca^{2+}	30.7	4.6	55.9	55.9	0.91	0.52	0.48
L*Zn^{2+}	19.9	4.3	35.5	35.0	0.99	0.50	0.50
L*Cd^{2+}	24.7	4.4	44.4	42.2	0.51	0.49	0.51
L*Hg^{2+}	2.2	2.6	3.0	5.6	1.87	0.34	0.66
			λ=1907nm				
L	39.1	4.7	71.6	63.8	0.89	0.53	0.47
L*Na$^+$	32.9	4.7	60.1	53.8	0.89	0.53	0.47
L*K$^+$	34.2	4.6	62.5	56.3	0.9.0	0.53	0.47
L*Mg^{2+}	18.1	4.3	32.2	32.0	0.99	0.50	0.50

L*Ca^{2+}	27.1	4.6	49.2	45.2	0.92	0.52	0.48
L*Zn^{2+}	17.5	4.3	31.1	31.2	1.0	0.50	0.50
L*Cd^{2+}	21.7	4.4	38.9	37.5	0.96	0.51	0.49
L*Hg^{2+}	2.1	0.6	2.8	5.3	1.89	0.35	0.65
			$\lambda=\infty$				
L	49.7	4.5	89.9	84.1	0.94	0.52	0.48
L*Na^{+}	39.2	4.4	70.4	67.8	0.96	0.50	0.50
L*K^{+}	41.0	4.4	73.6	71.0	0.97	0.51	0.49
L*Mg^{2+}	21.1	3.8	35.7	41.0	1.15	0.47	0.53
L*Ca^{2+}	31.9	4.2	56.4	56.9	1.00	0.50	0.50
L*Zn^{2+}	20.3	3.7	33.9	40.4	1.19	0.46	0.54
L*Cd^{2+}	24.9	3.9	42.5	48.0	1.12	0.47	0.53
L*Hg^{2+}	4.9	3.3	7.8	9.7	1.34	0.42	0.58

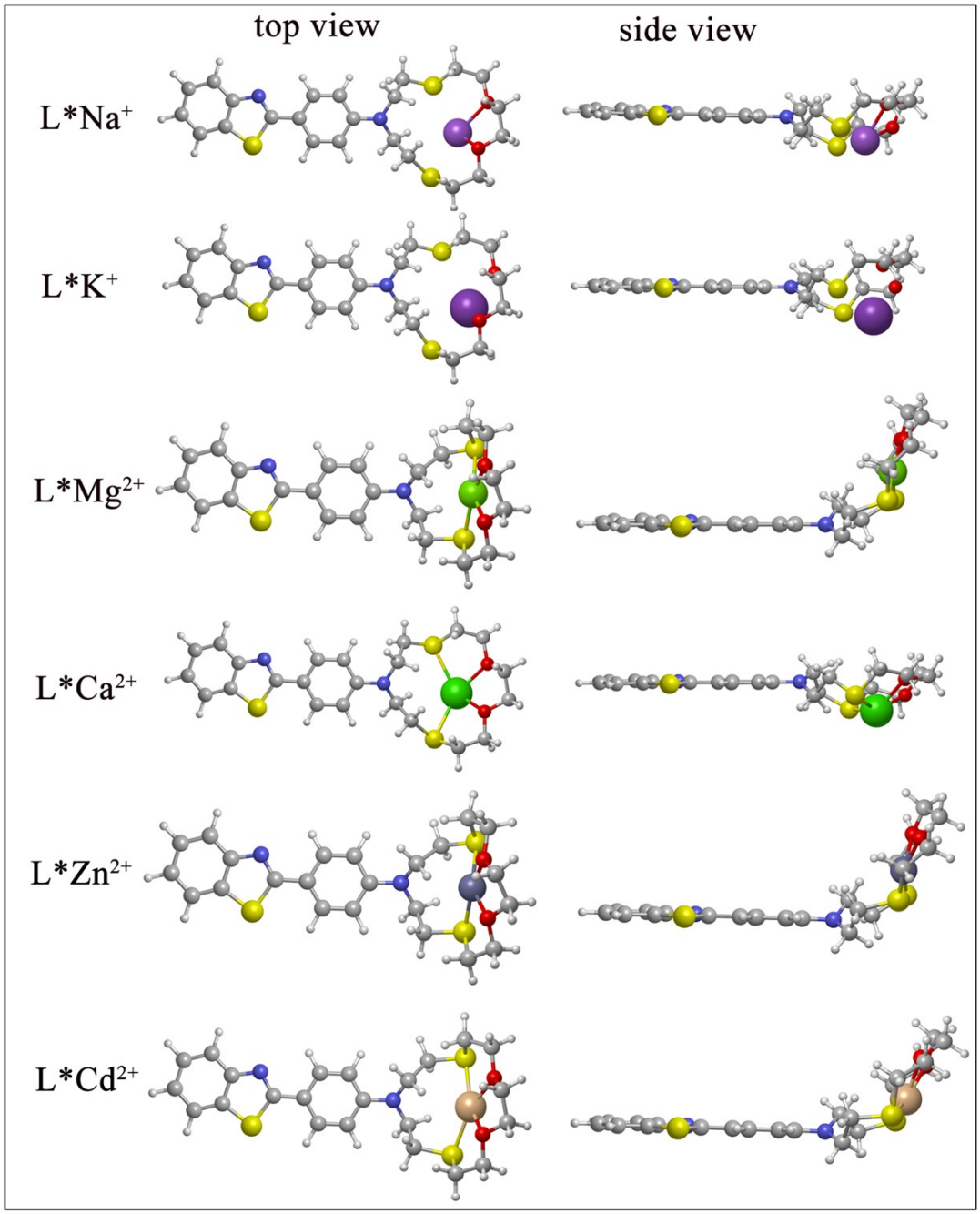

Figure S1. Optimized structures of **L*M** (M = Na^+, K^+, Mg^{2+}, Ca^{2+}, Zn^{2+}, and Cd^{2+}).